Analysis of Sinusoidal Interfacial Wrinkling of an Anisotropic Film Sandwiched Between Two Compliant Layers

J. W. Yang
Institute of Applied Mechanics,
School of Aerospace Engineering
and Applied Mechanics,
Tongji University,
Shanghai 200092, China

G. H. Nie[1]
Institute of Applied Mechanics,
School of Aerospace Engineering
and Applied Mechanics,
Tongji University,
Shanghai 200092, China
e-mail: ghnie@tongji.edu.cn

When a stiff film is bonded to a compliant layer and meanwhile encapsulated by another compliant layer on top, the film may form wrinkles under applied compressive stress. Inspired by the recent development of foldable circuit sealed in an encapsulating layer to improve bendability, unlike the wide study of surface wrinkling in a bilayer system, this paper presents a study of possible sinusoidal interfacial wrinkling in such sandwich system. The film is assumed to be anisotropic with arbitrary orientation of elastic axis while both layers are isotropic. A linear perturbation analysis is performed to predict critical membrane stress, wave number and equilibrium amplitude for the onset of interfacial wrinkles. The effect of parameters such as elastic axis orientation of the film and moduli, thicknesses, and Poisson's ratios of the layers on the wrinkling is evaluated in detail. The results show that compared to two compliant layers, the stiffer and thinner the film is, the smaller the values of both the critical stress and wave number for wrinkling will be. Especially, we illustrate three limiting cases: two layers both reach thick-layer limit, two layers both reach thin-layer limit and one layer reaches thick-layer limit while the other layer reaches thin-layer limit. Analytical solutions are obtained for first two cases and numerical solutions are plotted for the third case. It is found that as long as the thin-layer is near incompressible, the interfacial wrinkles can be suppressed. In addition, the equilibrium wave modes for the three limiting cases are also given. The resulting solutions for the sandwich system can be reduced to the classic solutions for a bilayer system.
[DOI: 10.1115/1.4027974]

Keywords: thin stiff film, compliant layers, anisotropic material, nonlinear plate theory, wrinkling instability

1 Introduction

Surface wrinkling instability has often been observed in thin film on compliant substrate systems under compressive stresses, which exhibits versatile intricate patterns with distinct features [1–6]. For many applications of such integrated material system, despite the undesirable fact that wrinkles may lead to failure of the system by delamination or fracture [7–9], the wrinkling patterns have a huge potential for various applications. For instance, wrinkles may be used as stretchable and foldable electronics [10–16], nanoscale/microscale surface patterning [2,4,17,18], smart adhesion [19], optical lens [20] or a new method to measure the material properties of thin films [21,22].

A thin stiff film (e.g., aluminum) can be thermally deposited at a high temperature on a thick compliant substrate (e.g., polydimethylsiloxane (PDMS), polystyrene (PS)) [23–26]. When the film/substrate bilayer system is cooled down, the large thermal mismatch between the metal and elastomer generates equibiaxial compressive stresses in the film. When a critical temperature is reached, the film starts to wrinkle. Depending on stress state and boundary conditions, the resulting wrinkling patterns may either show highly ordered features such as sinusoidal stripes, zigzag herringbone, hexagonal, checkerboard, or disordered labyrinth [5,25,27]. Some theoretical studies have also been developed to understand the formation of surface wrinkling [28]. Cerda and Mahadevan used scaling analysis to determine the critical condition for wrinkling for a stretched thin membrane [29,30]. Chen and Hutchinson [23,24], Huang and Suo [31,32], Im and Huang [33,34], and Huang [35] have calculated the critical wavelength and equilibrium amplitude of sinusoidal wrinkles by linear perturbation analysis. In addition, Jiang et al. studied the buckling of thin film on compliant substrate under finite deformation and also considered the finite width effect of thin film [13–15].

In the fabrication of stretchable and foldable devices, sandwich system is of particular importance. To avoid delamination of the circuit (film/layer system) and/or fracture of metal interconnects (film) under high bending, an additional encapsulating layer is introduced on top of the circuit to improve adhesion and alleviate the strain level because such layer/film/layer sandwich system shifts the neutral mechanical plane to the film plane [11]. For example, Kim et al. [11] have shown excellent applications that they successfully fabricated polyimide/single-crystalline silicon complementary metal-oxide semiconductor/polyimide (PI/Si-CMOS/PI) foldable circuit, which not only exhibit good electrical properties but also show remarkable bendability. However, recent studies show that the additional encapsulation may decrease the strechability of sandwiched system [36].

Theoretical studies of surface wrinkling of sandwich system may be traced back to half century ago when face wrinkling of a structured sandwich panel (face strut/core/face strut) was analyzed as a form of local elastic instability [37,38]. However, unlike the structured sandwich panel, we adopt the design of layer/film/layer sandwich system with the material model for film is more general, that is, a stiff film (e.g., composite material) of anisotropic elasticity with arbitrary elastic axis orientation is well bonded between two compliant layers (e.g., elastomers) of isotropic elasticity, which are in turn bonded to rigid supports, as shown in Fig. 1(*a*).

[1]Corresponding author.

Contributed by the Applied Mechanics Division of ASME for publication in the Journal of Applied Mechanics. Manuscript received May 26, 2014; final manuscript received July 6, 2014; accepted manuscript posted July 9, 2014; published online July 21, 2014. Editor: Yonggang Huang.

The film forms pattern of wrinkles when the compressive stress exceed critical stress, as shown in Fig. 1(*b*). The thicknesses of two layers are taken to be finite and can be varied by orders of magnitude.

In this paper we focus on analysis of sinusoidal interfacial wrinkling of an anisotropic stiff film sandwiched between two isotropic compliant layers. The paper is organized as follows. In Sec. 2, the von Karman-type nonlinear governing equations for the anisotropic elastic film with arbitrary elastic orientation are formulated. In Sec. 3, we perform linear perturbation analysis, from which the critical membrane stress, wave number and equilibrium amplitude for the onset of wrinkles with variations of elastic axis orientation of the film and moduli, thicknesses, and Poisson's ratios of the layers are numerically presented. In Sec. 4, we illustrate three special cases: two layers are both thick, two layers are both thin, and one layer is thick while the other layer is thin, respectively. Analytical expressions for the critical stress, wave number and wavelength can be derived in first two cases. The equilibrium wave modes for the three limiting cases are also obtained. Finally, some conclusions are drawn in Sec. 5.

2 Governing Equations for Anisotropic Elastic Film With Arbitrary Elastic Axis Orientation

According to the theory of linear elasticity, the stress and strain relation for anisotropic material can be written in form of the generalized Hooke's law

$$\sigma_{ij} = C_{ijkl}\varepsilon_{kl} \tag{1}$$

where $C_{ijkl} = C_{jikl} = C_{ijlk} = C_{klij}$ are 21 independent elastic constants and subscripts i, j, k, l take values of 1–3 (refer to the elastic axis coordinate). A set of three elastic axis of anisotropic material is shown in Fig. 2(*a*), which has an arbitrary orientation angle θ relative to the Cartesian coordinate. If there is an elastic symmetrical plane about z axis (3-direction in elastic axis coordinate), then the anisotropic model can be written in the symmetric matrix form of

$$\begin{bmatrix}\sigma_{11}\\ \sigma_{22}\\ \sigma_{33}\\ \sigma_{23}\\ \sigma_{13}\\ \sigma_{12}\end{bmatrix} = \begin{bmatrix} C_{11} & C_{12} & C_{13} & 0 & 0 & 2C_{16}\\ C_{12} & C_{22} & C_{23} & 0 & 0 & 2C_{26}\\ C_{13} & C_{23} & C_{33} & 0 & 0 & 2C_{36}\\ 0 & 0 & 0 & 2C_{44} & 2C_{45} & 0\\ 0 & 0 & 0 & 2C_{54} & 2C_{55} & 0\\ 2C_{16} & 2C_{26} & 2C_{36} & 0 & 0 & 2C_{66}\end{bmatrix}\begin{bmatrix}\varepsilon_{11}\\ \varepsilon_{22}\\ \varepsilon_{33}\\ \varepsilon_{23}\\ \varepsilon_{13}\\ \varepsilon_{12}\end{bmatrix} \tag{2}$$

The film is modeled as a thin elastic plate. The classic plate theory provides all 3-direction stress components equal to zero, i.e., $\sigma_{13} = \sigma_{23} = \sigma_{33} = 0$ [33]. Hence, the in-plane stress and strain relation reduces to

$$\begin{bmatrix}\sigma_{11}\\ \sigma_{22}\\ \sigma_{12}\end{bmatrix} = \begin{bmatrix}\bar{C}_{11} & \bar{C}_{12} & 2\bar{C}_{16}\\ \bar{C}_{12} & \bar{C}_{22} & 2\bar{C}_{26}\\ 2\bar{C}_{16} & 2\bar{C}_{26} & 2\bar{C}_{66}\end{bmatrix}\begin{bmatrix}\varepsilon_{11}\\ \varepsilon_{22}\\ \varepsilon_{12}\end{bmatrix} \tag{3}$$

where $\bar{C}_{rs} = C_{rs} - C_{r3}C_{s3}/C_{33}$, $r = 1, 2,$ or 6. For an isotropic elastic plate, the reduced elastic constants are $\bar{C}_{11} = \bar{C}_{22} = E_f/(1-\nu_f^2)$, $\bar{C}_{12} = E_f\nu_f/(1-\nu_f^2)$, $\bar{C}_{16} = \bar{C}_{26} = 0$, and $\bar{C}_{66} = E_f/[2(1+\nu_f)]$, where E_f and ν_f are Young's modulus and Poisson's ratio.

The stress–strain relation in Eq. (3) is respect to the elastic principal coordinates (1,2) which can be transformed to the elastic constants with respect to the Cartesian coordinates (x, y). The transformation formula for the stresses is as follows:

$$\begin{aligned}\sigma_{xx} &= \sigma_{11}\cos^2\theta + \sigma_{22}\sin^2\theta - 2\sigma_{12}\sin\theta\cos\theta\\ \sigma_{yy} &= \sigma_{11}\sin^2\theta + \sigma_{22}\cos^2\theta + 2\sigma_{12}\sin\theta\cos\theta\\ \sigma_{xy} &= \sigma_{11}\sin\theta\cos\theta - \sigma_{22}\sin\theta\cos\theta + \sigma_{12}(\cos^2\theta - \sin^2\theta)\end{aligned} \tag{4}$$

The strain components transformation has similar form as stress components transformation provided that the stress components are replaced with corresponding strain components. We inversely express the relation from strain components at Cartesian coordinate to strain components at elastic axis coordinate

$$\begin{aligned}\varepsilon_{11} &= \varepsilon_{xx}\cos^2\theta + \varepsilon_{yy}\sin^2\theta + 2\varepsilon_{xy}\sin\theta\cos\theta\\ \varepsilon_{22} &= \varepsilon_{xx}\sin^2\theta + \varepsilon_{yy}\cos^2\theta - 2\varepsilon_{xy}\sin\theta\cos\theta\\ \varepsilon_{12} &= -\varepsilon_{xx}\sin\theta\cos\theta + \varepsilon_{yy}\sin\theta\cos\theta + \varepsilon_{xy}(\cos^2\theta - \sin^2\theta)\end{aligned} \tag{5}$$

Substituting Eqs. (3) and (5) into Eq. (4), the elastic constants at Cartesian coordinates are obtained. For simplicity, here, we consider orthotropic material which has three elastic symmetrical planes. The material model can be rewritten as

$$\begin{bmatrix}\sigma_{xx}\\ \sigma_{yy}\\ \sigma_{xy}\end{bmatrix} = \begin{bmatrix}\bar{\bar{C}}_{11} & \bar{\bar{C}}_{12} & 2\bar{\bar{C}}_{16}\\ \bar{\bar{C}}_{12} & \bar{\bar{C}}_{22} & 2\bar{\bar{C}}_{26}\\ 2\bar{\bar{C}}_{16} & 2\bar{\bar{C}}_{26} & 2\bar{\bar{C}}_{66}\end{bmatrix}\begin{bmatrix}\varepsilon_{xx}\\ \varepsilon_{yy}\\ \varepsilon_{xy}\end{bmatrix} \tag{6}$$

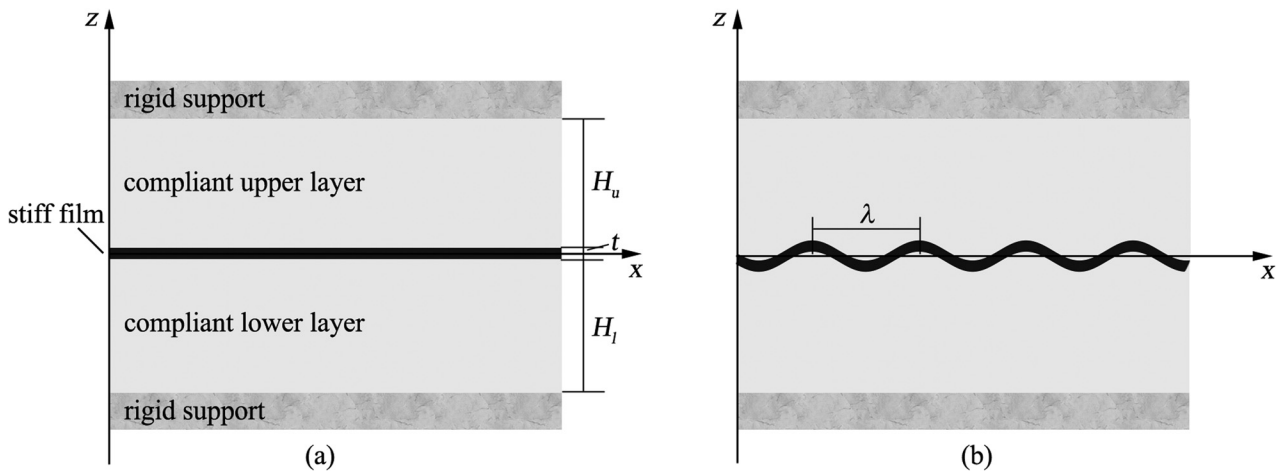

Fig. 1 (*a*) Schematics of undeformed sandwich system that a stiff film is in between of two finite-thickness compliant layers which in turn are bonded to rigid supports. (*b*) Deformed sandwich system that film forms interfacial wrinkles with wavelength described as λ and the wave number can be calculated as $k = 2\pi/\lambda$.

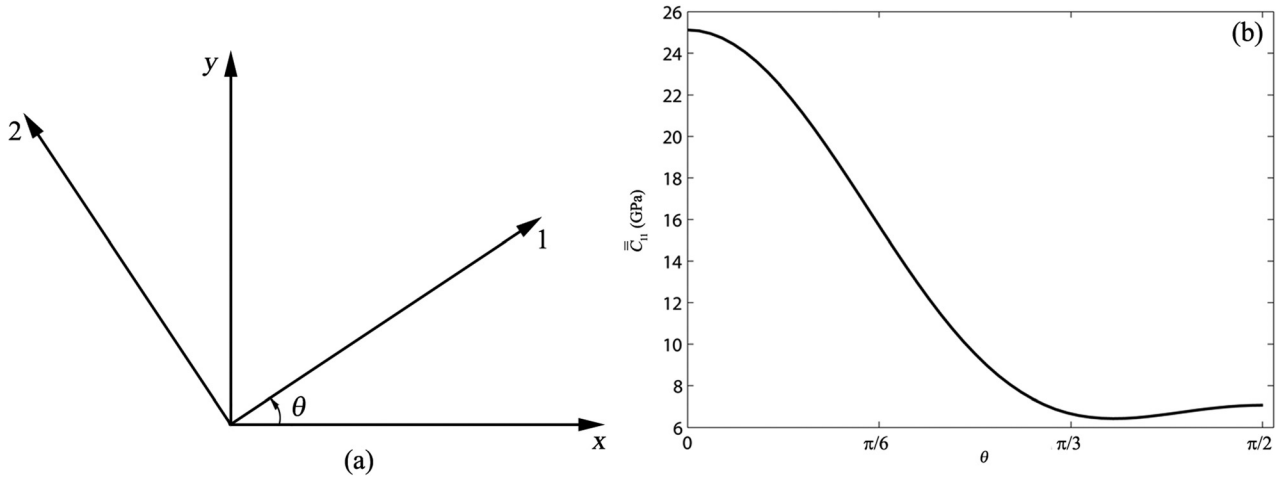

Fig. 2 (*a*) Schematics of in-plane elastic axis of anisotropic material labeled as 1, 2 and Cartesian coordinates as global coordinates labeled as *x*, *y*. The rotate angle between the two set of coordinates is θ, which is also defined as elastic axis orientation angle. (*b*) The in-plane modulus of film in *x* direction with variation of θ.

where the elastic constants at Cartesian coordinates can be expressed as

$$\begin{aligned}
\bar{\bar{C}}_{11} &= \bar{C}_{11}\cos^4\theta + 2(\bar{C}_{12}+2\bar{C}_{66})\sin^2\theta\cos^2\theta + \bar{C}_{22}\sin^4\theta \\
\bar{\bar{C}}_{12} &= (\bar{C}_{11}+\bar{C}_{22}-4\bar{C}_{66})\sin^2\theta\cos^2\theta + \bar{C}_{12}(\sin^4\theta+\cos^4\theta) \\
\bar{\bar{C}}_{22} &= \bar{C}_{11}\sin^4\theta + 2(\bar{C}_{12}+2\bar{C}_{66})\sin^2\theta\cos^2\theta + \bar{C}_{22}\cos^4\theta \\
2\bar{\bar{C}}_{16} &= 2(\bar{C}_{11}-\bar{C}_{12}-2\bar{C}_{66})\sin\theta\cos^3\theta \\
&\quad + 2(\bar{C}_{12}-\bar{C}_{22}+2\bar{C}_{66})\sin^3\theta\cos\theta \\
2\bar{\bar{C}}_{26} &= 2(\bar{C}_{11}-\bar{C}_{12}-2\bar{C}_{66})\sin^3\theta\cos\theta \\
&\quad + 2(\bar{C}_{12}-\bar{C}_{22}+2\bar{C}_{66})\sin\theta\cos^3\theta \\
2\bar{\bar{C}}_{66} &= 2(\bar{C}_{11}-2\bar{C}_{12}+\bar{C}_{22}-2\bar{C}_{66})\sin^2\theta\cos^2\theta \\
&\quad + 2\bar{C}_{66}(\sin^4\theta+\cos^4\theta)
\end{aligned}$$

Since the elastic stiffnesses $\bar{\bar{C}}_{16}$ and $\bar{\bar{C}}_{26}$ are negligible compared to other elastic stiffnesses [39], we will not consider the coupling between stretch and shear, and consequently set $\bar{\bar{C}}_{16}$ and $\bar{\bar{C}}_{26}$ equal to zero. The stress–strain relation can be further simplified as

$$\begin{bmatrix}\sigma_{xx}\\ \sigma_{yy}\\ \sigma_{xy}\end{bmatrix} = \begin{bmatrix}\bar{\bar{C}}_{11} & \bar{\bar{C}}_{12} & 0\\ \bar{\bar{C}}_{12} & \bar{\bar{C}}_{22} & 0\\ 0 & 0 & 2\bar{\bar{C}}_{66}\end{bmatrix}\begin{bmatrix}\varepsilon_{xx}\\ \varepsilon_{yy}\\ \varepsilon_{xy}\end{bmatrix} \tag{7}$$

In the flat state, let the strain components in the film be ε^0_{xx}, ε^0_{yy}, and ε^0_{xy}. In the wrinkling state, let the deflection of the film be w, and the in-plane displacements be u_x and u_y, the Lagrangian strain components in the film can be written as

$$\begin{aligned}
\varepsilon_{xx} &= \varepsilon^0_{xx} + \frac{\partial u_x}{\partial x} + \frac{1}{2}\left(\frac{\partial w}{\partial x}\right)^2 \\
\varepsilon_{yy} &= \varepsilon^0_{yy} + \frac{\partial u_y}{\partial y} + \frac{1}{2}\left(\frac{\partial w}{\partial y}\right)^2 \\
\varepsilon_{xy} &= \varepsilon^0_{xy} + \frac{1}{2}\left(\frac{\partial u_x}{\partial y} + \frac{\partial u_y}{\partial x}\right) + \frac{1}{2}\left(\frac{\partial w}{\partial x}\right)\left(\frac{\partial w}{\partial y}\right)
\end{aligned} \tag{8}$$

where the first term represents prestrain, the second term represents in-plane displacement gradient, and the third term represents rotation caused by the deflection.

Similar to von Karman nonlinear plate theory [40], we can obtain the equilibrium equations for the anisotropic elastic film with arbitrary elastic orientation

$$\begin{aligned}
&\frac{t^3}{12}\left[\bar{\bar{C}}_{11}\frac{\partial^4 w}{\partial x^4} + \left(2\bar{\bar{C}}_{12}+4\bar{\bar{C}}_{66}\right)\frac{\partial^4 w}{\partial x^2\partial y^2} + \bar{\bar{C}}_{22}\frac{\partial^4 w}{\partial y^4}\right] \\
&\quad - t\left(\sigma_{xx}\frac{\partial^2 w}{\partial x^2} + 2\sigma_{xy}\frac{\partial^2 w}{\partial x\partial y} + \sigma_{yy}\frac{\partial^2 w}{\partial y^2}\right) = \Delta p
\end{aligned} \tag{9}$$

$$\begin{aligned}
\frac{\partial \sigma_{xx}}{\partial x} + \frac{\partial \sigma_{xy}}{\partial y} &= \frac{T_x}{t} \\
\frac{\partial \sigma_{xy}}{\partial x} + \frac{\partial \sigma_{yy}}{\partial y} &= \frac{T_y}{t}
\end{aligned} \tag{10}$$

where $\Delta p = p_u - p_l$ is the pressure (negative normal direction) difference exerted by upper and lower layers. Following the justification of Ref. [41], we safely remove the resultant shear stress component T_x and T_y at the interface between film and layers in Eq. (10). Hence, σ_{xx} and σ_{yy} are uniform in the film when σ_{xy} is absent.

3 Linear Perturbation Analysis

The lateral deflection of the film takes the sinusoidal form

$$w = A\cos(kx) \tag{11}$$

where k is wave number and A is amplitude. Using Eq. (9), the one dimensional linearized bucking form can be written as

$$\frac{t^3}{12}\bar{\bar{C}}_{11}\frac{\partial^4 w}{\partial x^4} - t\sigma^0_{xx}\frac{\partial^2 w}{\partial x^2} = \Delta p \tag{12}$$

where σ^0_{xx} is the membrane stress in the film caused by prestrain ε^0_{xx}. Inserting Eq. (11) into Eq. (12), yields

$$\frac{t^3}{12}k^4\bar{\bar{C}}_{11}w + t\sigma_{xx}k^2 w = \Delta p \tag{13}$$

in which Δp can be determined from p_u and p_l which are obtained by solving the boundary value problem in-plane strain condition. The boundary conditions are considered as follows: the lower layer whose top surface and upper layer whose bottom surface are subjected to displacement $w = A\cos(kx)$ and zero shear stress, while the lower layer whose bottom surface and upper layer

whose top surface are perfectly constrained to the rigid supports. The boundary value problem can be solved by separation of Airy stress function in the form of $F(x,z) = f(z)\cos(kx)$, one can obtain the analytical solutions (see the Appendix for details) as

$$p_u(kH_u, \nu_u) = g_u \overline{E}_u kw \tag{14}$$

$$p_l(kH_l, \nu_l) = g_l \overline{E}_l kw \tag{15}$$

where u and l denote upper layer and lower layer, respectively, and g_u, g_l can be found in Eq. (A12). Combination of Eqs. (13)–(15) gives

$$\frac{\sigma^0_{xx}}{\overline{\overline{C}}_{11}} = \frac{g_u \dfrac{\overline{E}_u}{\overline{\overline{C}}_{11}} - g_l \dfrac{\overline{E}_l}{\overline{\overline{C}}_{11}} - \dfrac{(kt)^3}{12}}{kt} \tag{16}$$

Enforcing the first derivative of Eq. (16) with respect to k equals to zero

$$\frac{\partial \sigma^0_{xx}}{\partial k} = 0 \tag{17}$$

Thus, the critical wave number k_c is the solution of Eq. (17) and the critical membrane stress $\sigma^c_{xx} = \sigma^c_{xx}(k_c)$. Here, the solution is provided for the case that $-\sigma^0_{xx} > -\sigma^c_{xx}$. Since Eq. (17) is highly nonlinear, it is difficult to obtain explicit solutions for k_c and σ^c_{xx}. Instead, we numerically plot normalized membrane stress $\sigma^0_{xx}/\overline{\overline{C}}_{11}$ as a function of normalized wave number kt with variations of elastic axis orientation of the film and moduli, thicknesses, and Poisson's ratios of two layers in Fig. 3. The critical membrane stress can be found by searching the extreme value on the curve (the dash line in Fig. 3(*a*) as an example).

Figure 3(*a*) plots normalized membrane stress $\sigma^0_{xx}/\overline{\overline{C}}_{11}$ as a function of normalized wave number kt with variations of moduli of layers. Because the upper and lower layer is symmetric, without loss of generality, we fix the modulus of lower layer and vary the modulus of upper layer. It is noted that for certain moduli of the film and lower layer (e.g., $E_l = 1$ GPa and $\overline{\overline{C}}_{11} = 25.12$ GPa, dot lines), as the modulus of upper layer decreases until vanishes (recovers to a bilayer system), the critical membrane stress and wave number both decrease. Moreover, if the modulus of lower layer further decreases ($E_l = 0.01$GPa) and the modulus of upper layer is kept unchanged, both the critical wave number and membrane stress further drop dramatically (dotted–dashed lines). In the limiting case, when both layers vanish, there is no extreme value. The film deforms homogeneously and is unable to form wrinkles due to loss of constraint (solid line). Figure 3(*b*) shows normalized membrane stress $\sigma^0_{xx}/\overline{\overline{C}}_{11}$ as a function of normalized wave number kt with variations of thicknesses of layers. As thickness of the upper layer decreases ($H_u = 100t$ drops to $0.1t$) while the thicknesses of film t and the lower layer $H_l = 0.1t$ are fixed (dotted lines), $H_l = t$ (dotted–dashed lines) and $H_l = 10t$ (solid lines), respectively, both the critical wave number and membrane stress increase. When the thickness of film is ten times, the thickness of upper and lower layers (e.g., $H_u = H_l = 0.1t$, dotted line), $\sigma^c_{xx}/\overline{\overline{C}}_{11} = -0.2$ and $k_c t = 1.1$, which is almost ten times the critical membrane stress and wave number for the case $H_u = H_l = 10t$ (solid line). In addition, we also note that for $H_l = t$, the critical condition is almost the same when the thickness of the upper layer is $10t$ and $100t$, which means thick-layer limit of the upper layer is $10t$ when $H_l = t$. The Poisson's ratios of layers reflect

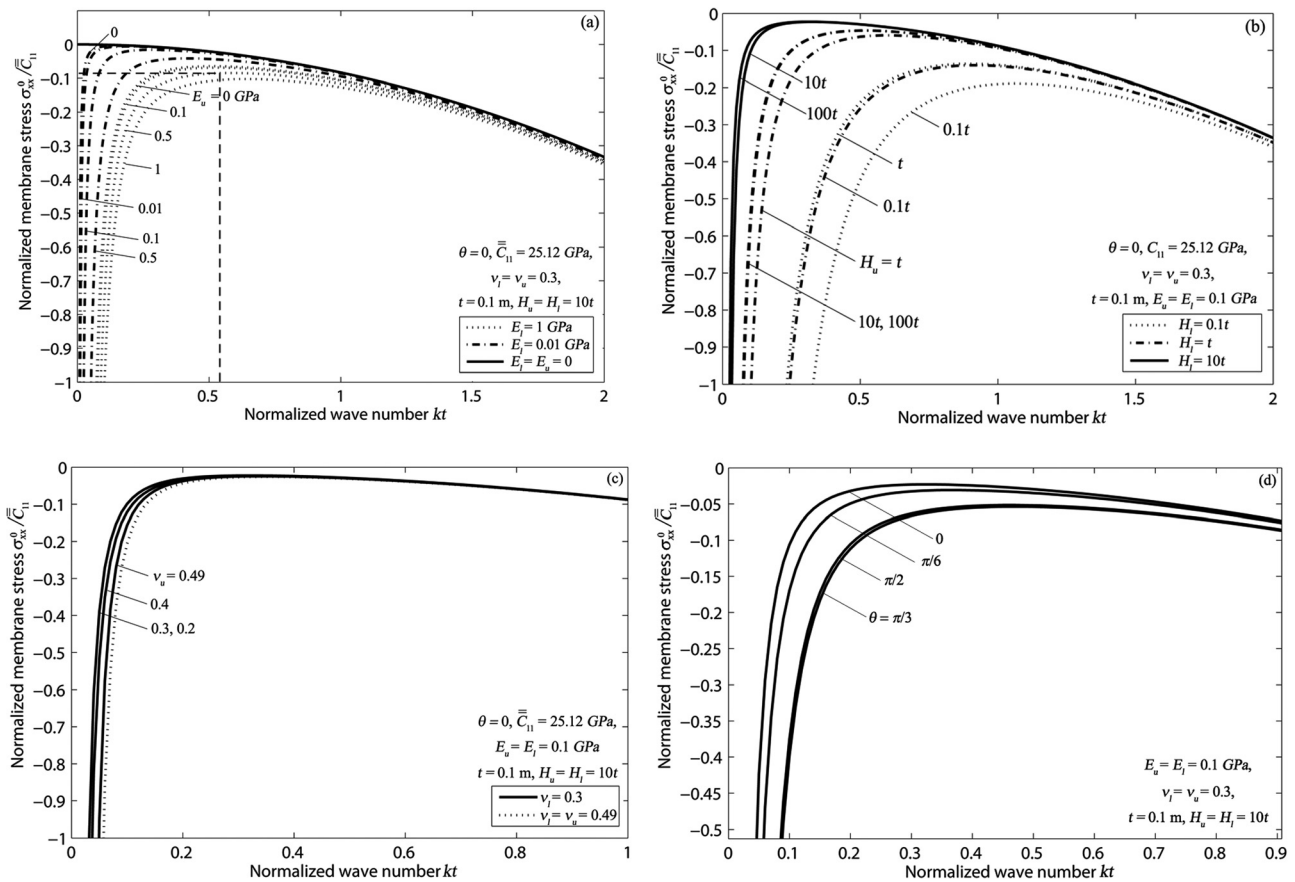

Fig. 3 The normalized membrane stress as a function of normalized wave number with variations of two layers' (*a*) moduli, (*b*) thicknesses, (*c*) Poisson's ratios, and (*d*) elastic axis orientation angle of the film

compressibility of material. The larger Poisson's ratio seems to stiffen the layers, giving rise to higher critical membrane stress and wave number (Fig. 3(*c*)). The extreme critical condition is reached when both layers are near incompressible (dot line). Moreover, the elastic axis orientation of the film only affects the modulus. Figure 2(*b*) plots the in-plane modulus of film in x direction with variation of θ. Since $\theta = 0$ and $\theta = 1.162$ correspond to maximum and minimum values of modulus, respectively, hence, both critical membrane stress and wave number reach minimum values when $\theta = 0$ and reach their maximum values when $\theta = 1.162$, the tendency is shown in Fig. 3(*d*). In summary, it is clear that interfacial wrinkles are more easily to form when the film is stiffer and thinner to both layers.

Next, we turn to determine the equilibrium amplitude of interfacial wrinkles. The amplitude of wrinkles in equilibrium can be captured by the constraint between the film and the two layers, which means the horizontal deformation of the film should be compatible with the deformations of the two layers, namely, $\int_0^{2\pi/k} \partial\left(u_x - u_x^0\right)/\partial x\, dx = 0$. Under combination of Eq. (7) with Eq. (8), we can further write

$$\frac{1}{\overline{\overline{C}}_{11}}\left(-\sigma_{xx}^0 + \sigma_{xx}^c\right) = \frac{k_c}{4\pi}\int_0^{\frac{2\pi}{k_c}} \left(\frac{dw}{dx}\right)^2 dx = \frac{k_c^2}{4}A^2 \tag{18}$$

The expression for amplitude can be written as

$$A = \frac{2}{k_c}\left(\frac{-\sigma_{xx}^0 + \sigma_{xx}^c}{\overline{\overline{C}}_{11}}\right)^{\frac{1}{2}} \tag{19}$$

In Fig. 4, we fix modulus and thickness of the film ($E_l = 10^{-2}$ GPa and 10^{-4}GPa, respectively) and plot the critical normalized membrane stress $\sigma_{xx}^c/\overline{\overline{C}}_{11}$, wave number $k_c t$, and the equilibrium amplitude A/t as a function of thickness ratio of layers to the film, H/t ($H = H_u = H_l$), with variations of both moduli and Poisson's ratios of the layers for $\nu_u = \nu_l = 0.3$ (left column) and $\nu_u = 0.1, \nu_l = 0.49$ (right column), respectively. As seen from first two rows in Fig. 4, it is readily to see that as thickness ratio of the layer to film increases or modulus of upper layer decrease (for a certain modulus of lower layer), interfacial wrinkles set in at the smaller value of the membrane stress and wave number. It is also noted that the normalized amplitude has two plateaus with variation of H/t, which are associated with the thick-layer limit and thin-layer limit. When the value of H/t goes beyond the range of 10–100, it seems that the layers' thicknesses approach the thick-layer limit. Both the membrane stress and wave number keep constant and have minimum value. For example, in thick-layer limit, when $E_l = 10^{-4}$ GPa, $E_u = 10^{-5}$ GPa, interfacial wrinkles set in when the membrane stress only exceeds about -10^{-4}, the wavelength ($k = 2\pi/\lambda$) is hundred times the thickness of film and the equilibrium amplitude is in the order of film thickness. Furthermore, when E_u drops down to 10^{-5} GPa and 10^{-3} GPa for the case $E_l = 10^{-4}$ GPa and $E_l = 10^{-2}$ GPa, respectively, the existence of upper layer becomes unimportant and the sandwich system resembles the bilayer system. However, in the thin layers limit, the constraints of rigid support at boundary of both layers take effects which strongly restrict the deformation. As a result, both layers get stiffer. Meanwhile, if the layers are also near incompressible, they become even stiffer (see Fig. 3(*c*)). Consequently, both the critical membrane stress and wave number have even higher values and the equilibrium amplitude has a smaller value.

The effects of elastic axis orientation angle of the film on the critical membrane stress and wave number with variations of moduli, thicknesses, and Poisson's ratios of the layers are displayed in Fig. 5. Due to the same mechanism that the stiffer film has lower critical membrane stress and wave number, we expect that for certain set of moduli, thicknesses, and Poisson's ratios of the layers, the smallest and biggest critical membrane stresses and wave numbers occur when maximum ($\theta = 0, \overline{\overline{C}}_{11} = 25.12$ GPa) and minimum ($\theta = 1.162, \overline{\overline{C}}_{11} = 6.425$ GPa) moduli of film are reached. Nevertheless, if the moduli for both layers become smaller (or Poisson's ratios become smaller), or thicknesses become bigger, the difference between the maximum and minimum values is smaller and the curves appear to be flatter.

4 Three Limiting Cases

This section focuses on three limiting cases: two layers both reach thick-layer limit (e.g., Si-CMOS circuit that uses a dual neutral plane design), two layers both reach thin-layer limit, and one layer reaches thick-layer limit while the other layer reaches thin-layer limit (e.g., a metal film deposited on thick substrate sealed by a thin layer), which may find diverse engineering applications.

4.1 Two Layers Both Reach Thick-Layer Limit. Since both layers are thick compared to the film, $H_u/t \to \infty, H_l/t \to \infty$, the only length scale in the problem is wrinkle wavelength, so g_u and g_l must be constant. Equation (A12) gives $g_u = -1/2$ and $g_l = 1/2$ which are substituted back to Eq. (16). Solve Eq. (17) for $k_c t$

$$k_c t = \left[\frac{3\left(\overline{E}_u + \overline{E}_l\right)}{\overline{\overline{C}}_{11}}\right]^{\frac{1}{3}} \tag{20}$$

which is the critical normalized wave number of the interfacial wrinkles between two thick layers. The corresponding critical stress for the wrinkling can be obtained by taking Eq. (20) back to Eq. (16)

$$\frac{\sigma_{xx}^c}{\overline{\overline{C}}_{11}} = -\frac{1}{4}\left[\frac{3\left(\overline{E}_u + \overline{E}_l\right)}{\overline{\overline{C}}_{11}}\right]^{\frac{2}{3}} \tag{21}$$

Inserting Eq. (20) and Eq. (21) into Eq. (19), the equilibrium amplitude is

$$\frac{A}{t} = \left(\frac{\sigma_{xx}^0}{\sigma_{xx}^c} - 1\right)^{\frac{1}{2}} \tag{22}$$

Relations (20) and (21) show that both the critical membrane stress and wave number depend on the modulus ratio of the film and layers, and the latter also depends on the thickness of the film. Further, they are independent of the prestress. Relation (22) indicates the wrinkle amplitude exists only when the prestress exceeds the critical stress.

4.2 Two Layers Both Reach Thin-Layer Limit. In contrary to the first case, if thicknesses of two layers approach zero, which are thin-layer limit, we take $H_u/t \to 0, H_l/t \to 0$, which gives $g_u = -\left[(1-\nu_u)^2/(1-2\nu_u)\right](kH_u)^{-1}$, and $g_l = \left[(1-\nu_l)^2/(1-2\nu_l)\right](kH_l)^{-1}$. Solution for Eq. (17) gives

$$k_c t = \left[\frac{12t(1-\nu_u)^2\overline{E}_u}{H_u(1-2\nu_u)\overline{\overline{C}}_{11}} + \frac{12t(1-\nu_l)^2\overline{E}_l}{H_l(1-2\nu_l)\overline{\overline{C}}_{11}}\right]^{\frac{1}{4}} \tag{23}$$

which is the critical normalized wave number for the interfacial wrinkles between two thin layers. Substituting Eq. (23) back to Eq. (16) yields the corresponding critical stress for the wrinkling

$$\frac{\sigma_{xx}^{c}}{\overline{\overline{C}}_{11}} = -\left[\frac{(1-\nu_u)^2\overline{E}_u t}{3(1-2\nu_u)\overline{\overline{C}}_{11}H_u} + \frac{(1-\nu_l)^2\overline{E}_l t}{3(1-2\nu_l)\overline{\overline{C}}_{11}H_l}\right]^{\frac{1}{2}} \tag{24}$$

Inserting Eqs. (23) and (24) into Eq. (19) gives the equilibrium amplitude as

$$\frac{A}{t} = \left[\frac{2}{3}\left(\frac{\sigma_{xx}^{0}}{\sigma_{xx}^{c}} - 1\right)\right]^{\frac{1}{2}} \tag{25}$$

Unlike the thick layers limit, relations (23) and (24) show that the critical membrane stress and wave number depend not only on modulus ratio of the film and layers but also Poisson's ratios of both layers and thicknesses of all the three layers. The equilibrium amplitude differs by a precoefficient, $\sqrt{6}/3$. Again, the wrinkle amplitude exists only when the prestress exceeds the critical stress.

The relations (20)–(25) are indicated in Fig. 4. It is interesting to note that Eq. (24) excludes the incompressibility ($\nu = 0.5$). However, g_u and g_l in Eq. (A12) do not have this limitation and the limit value can be still obtained by putting $\nu = 0.5$. Since this procedure has been discussed elsewhere [41], we will not discuss in this paper. Rather, we simply let $\nu = 0.49$ as near incompressibility in Fig. 4. Attention is paid that for thin-layer limit, the power relation of Eq. (23) is from 1/4 to near 1/2 and the power relation of Eq. (24) is from 1/2 to near 1, while for thick-layer limit, no adjustment is needed. Moreover, relations (20)–(25) are analogues to the results of sinusoidal wrinkling of film on a thick or thin substrate produced by Refs. [24] and [41] but add one more term contributed from upper layer, and the expression for the equilibrium amplitude is exactly the same. Furthermore, if one

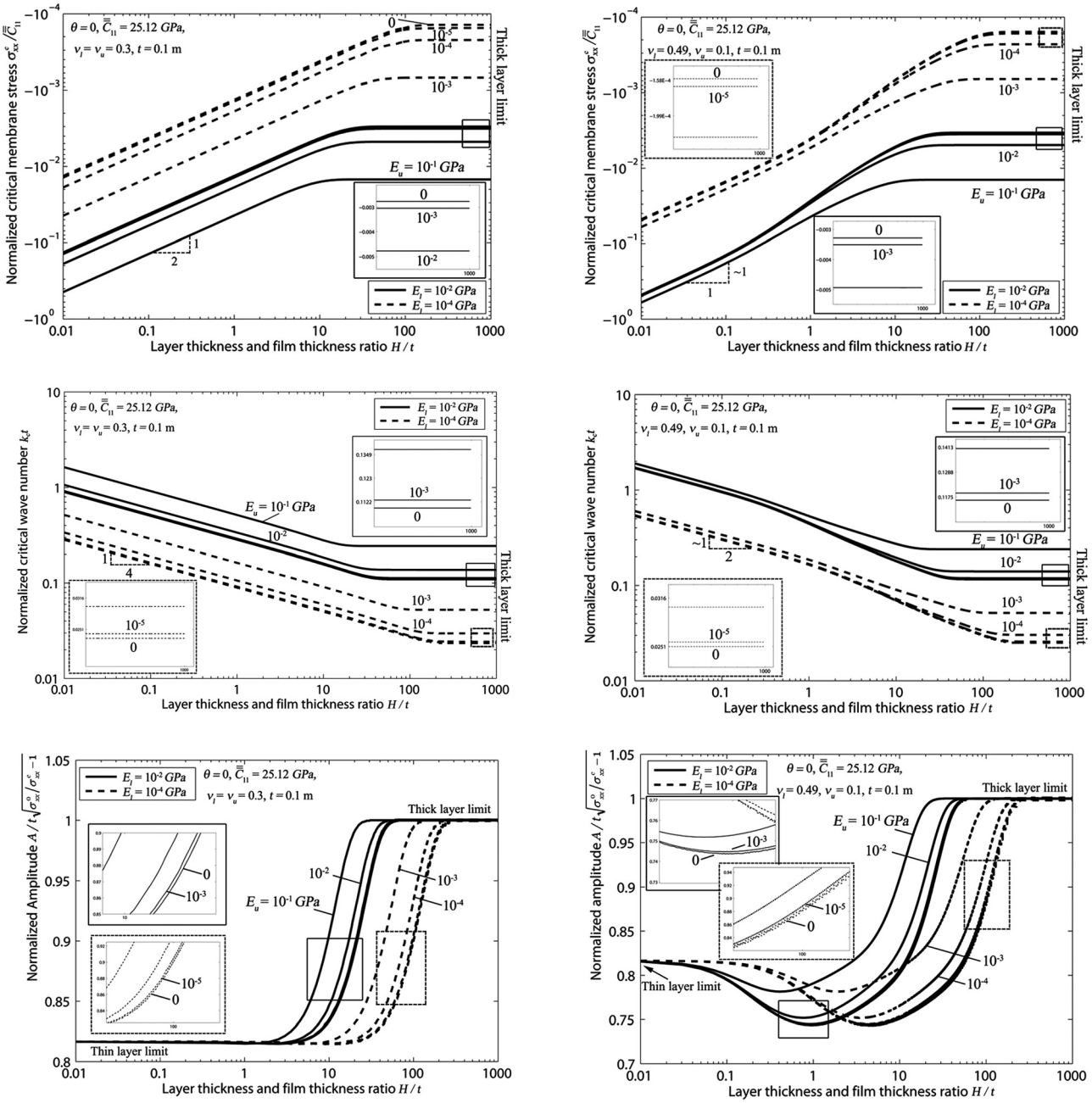

Fig. 4 The critical normalized membrane stress, wave number and the equilibrium amplitude as a function of thicknesses ratio of the layers and film with variations of both layers' moduli. Left column shows $\nu_u = \nu_l = 0.3$ and right column shows $\nu_u = 0.1$, $\nu_l = 0.49$. The insets show the close-up view of rectangular region in the figure.

of the layers is absent (e.g., $E_u = 0$), the sandwich system reduces to a bilayer system. When the film is isotropic, one can obtain $\overline{\overline{C}}_{11} = \overline{E}_f$ and relations (20)–(25) recover the classic relations for the thick-substrate limit and thin-substrate limit [41].

4.3 One Layer Reaches Thick-Layer Limit While the Other Layer Reaches Thin-Layer Limit. It may be another possible engineering application that a film lays on a thick substrate and is in turn covered by a thin skin on its top. In this case, we take the upper layer to be thin and the lower layer to be thick. The reverse case is similar. Likewise, $g_u = -[(1-\nu_u)^2/(1-2\nu_u)](kH_u)^{-1}$ and $g_l = 1/2$. The analytical solution can be obtained by the same procedure described in above two cases, but the expression is quite lengthy and complicated. Normalized critical membrane stress $\sigma^c_{xx}/\overline{\overline{C}}_{11}$ and normalized critical wave number $k_c t$ as functions of elastic axis orientation angle of film with variations of moduli and Poisson's ratios of the layers are displayed in Fig. 6.

The smallest and biggest value of critical membrane stresses and wave numbers are still found when maximum and minimum moduli of film are reached where $\theta = 0$ and $\theta = 1.162$, respectively. In comparison to the thick layers limit and thin layers limit (relations (20), (21), (23), and (24)) by fixing the same material properties of film and both layers (see Fig. 6 for details), we find that the critical membrane stress and wave number are smaller than that for thin layers limit but bigger than that for thick layers limit. For example, when $\theta = 0, E_l = E_u = 10^{-2}$ GPa, ν_l

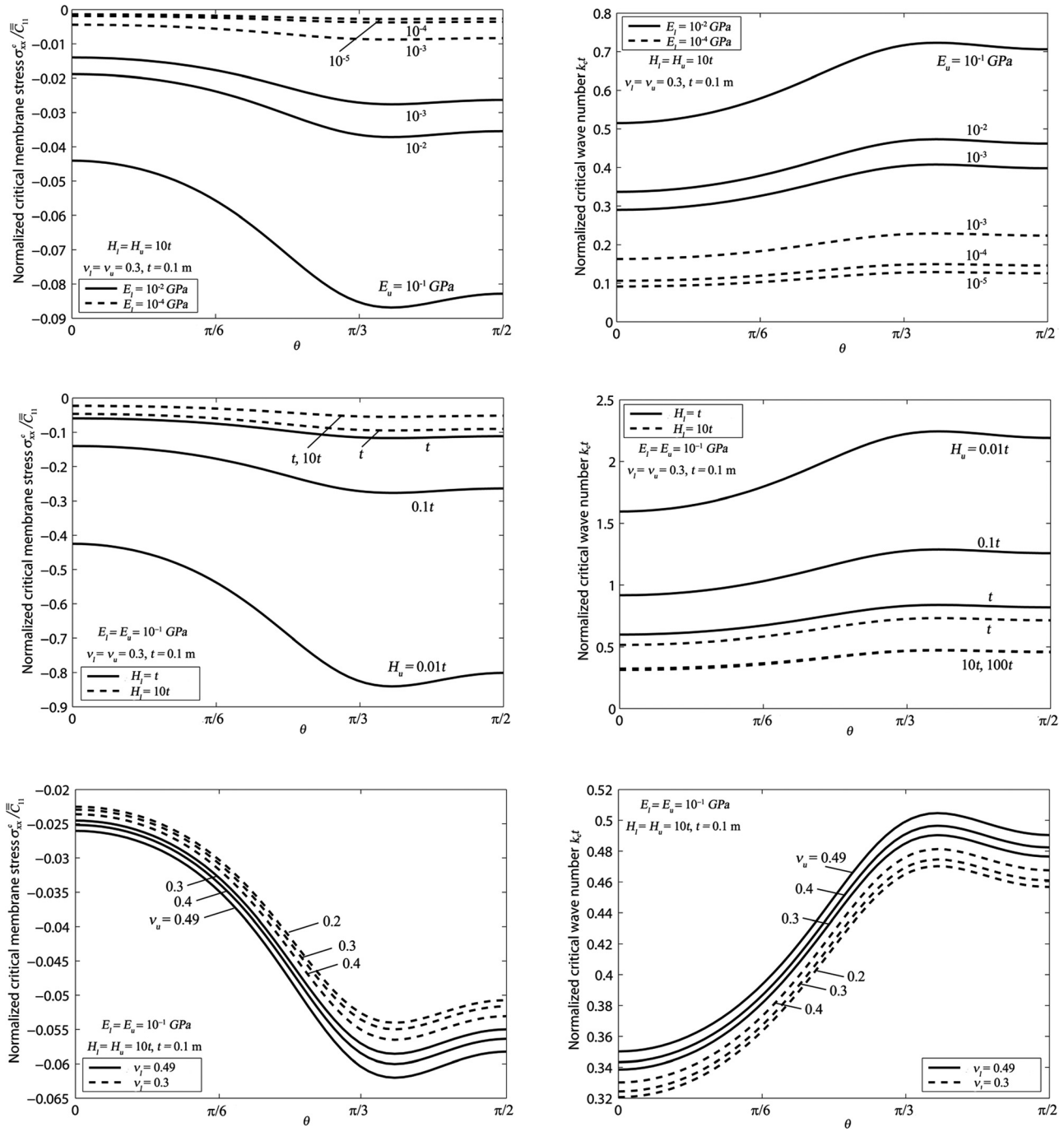

Fig. 5 The effects of elastic axis orientation angle of film on the critical membrane stress and wave number with variations of moduli, thicknesses, and Poisson's ratios of both layers

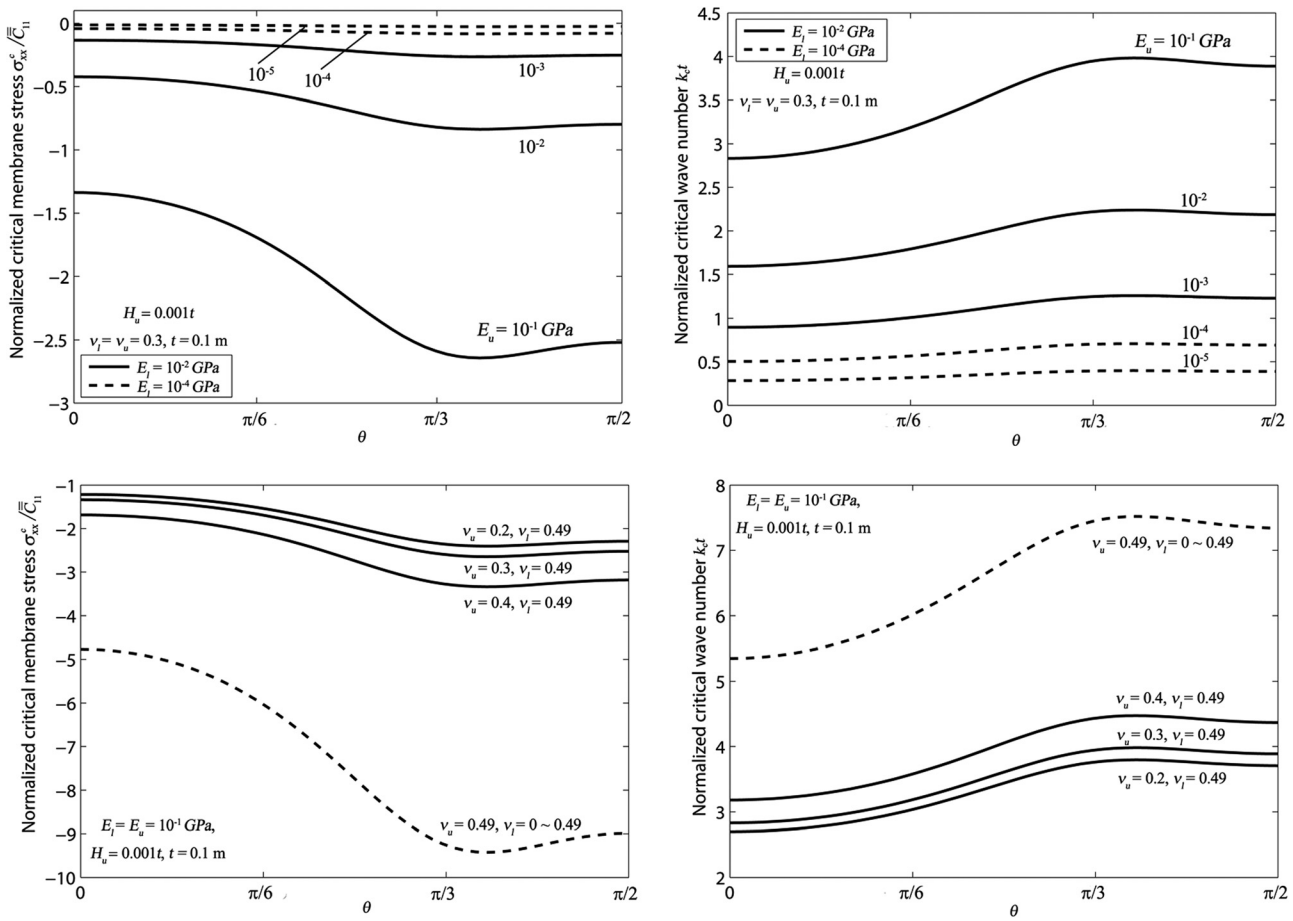

Fig. 6 The normalized critical membrane stress and wave number as a function of elastic axis orientation angle of film with variations of moduli and Poisson's ratios of both layers for a film sandwiched between a thick layer and a thin layer

$= \nu_u = 0.3, t = 0.1\text{m}, H_u = 0.001t$, the critical membrane stress and wave number for a film between thick and thin layers are -0.4228 and 1.593, respectively; for thick layers limit are -0.0048 and 1.379, respectively; for thin layers limit are -0.5977 and 1.894, respectively. This implies that the wrinkles are extremely difficult to form as long as one of the layers is very thin since the critical membrane stress for thin layers limit is hundred times bigger than that for thick layers limit. The reason is that the constraint from rigid supports is quite strong for a thin layer so that constrains the interfacial deformation. As a result, a large value of energy is required to wrinkle a thin layer, so is the larger critical membrane stress. Nevertheless, the weak constraint from rigid supports on interface between the film and thick layer needs only a small energy to wrinkle the surface of a thick layer while the remaining part of thick layer far from the surface is unaffected. Consequently, only a small critical membrane stress is needed to cause wrinkles for film between the thick layers. Moreover, we find if the lower thick layer is near incompressible, the higher the Poisson's ratio of upper thin layer is, the higher critical membrane stress and wave number will be (solid lines in the last row of Fig. 6). In contrary, for the reverse case, an interesting feature is captured. As long as the upper thin film is near incompressible, the critical membrane stress and wave number are unchanged no matter the lower layer is compressible or incompressible, and both values are far larger than the former case (dash line in the last row of Fig. 6). This is because the constraint by the stiffened thin layer enhanced by incompressibility is so overwhelming that compressibility for the thick layer appears insignificant. This feature may be used as a method to suppress the surface wrinkling. In addition, we also plot the equilibrium wave modes for the three limiting cases where $\overline{E}_u/\overline{\overline{C}}_{11} = \overline{E}_l/\overline{\overline{C}}_{11} = 0.01$, $t/H_u = t/H_l = 10$, $\nu_u = \nu_l = 0.3$, $\sigma^0_{xx}/\overline{\overline{C}}_{11} = -0.5$, as shown in Fig. 7. It is obvious to see that when both layers are thick, the wave number is small ($kt = 0.3915$) and the amplitude is large ($A/t = 3.4712$). When both layers are thin, the wave number is large ($kt = 1.3094$) and the amplitude is small ($A/t = 0.7069$). If one layer is thick and the other is thin, the wave number ($kt = 1.1075$) and amplitude ($A/t = 0.9782$) is in between the values, respectively, for the above two case.

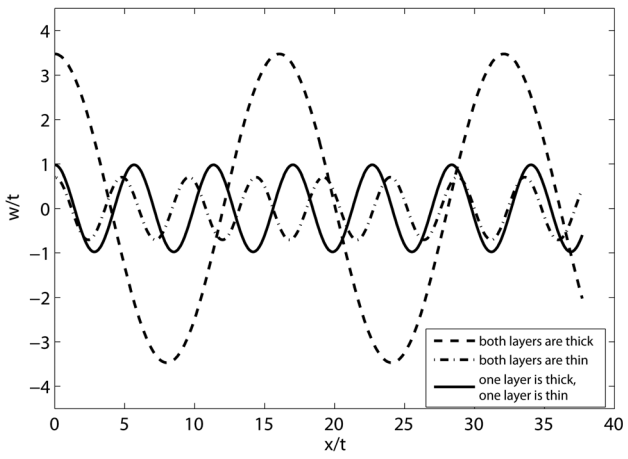

Fig. 7 The equilibrium wave modes for the three limiting cases when $\overline{E}_u/\overline{\overline{C}}_{11} = \overline{E}_l/\overline{\overline{C}}_{11} = 0.01$, $t/H_u = t/H_l = 10$, $\nu_u = \nu_l = 0.3$, $\sigma^0_{xx}/\overline{\overline{C}}_{11} = -0.5$

5 Conclusions

The paper presents a theoretical analysis of interfacial sinusoidal wrinkling of anisotropic film sandwiched between two compliant layers. A linear perturbation analysis is conducted to determine the critical membrane stress and wave number as well as equilibrium amplitude with variations of elastic axis orientation of the film and moduli, thicknesses, and Poisson's ratios of the two layers. Interfacial wrinkles set in when the membrane stress reaches its critical value. Analysis of effect of various parameters on wrinkling is done. The results show that as the film becomes much stiffer and thinner than that of the two layers, the wrinkles set in at a smaller critical membrane stress and wave number. In addition, we illustrate three limiting cases: two layers both reach thick-layer limit, two layers both reach thin-layer limit and one layer reaches thick-layer limit while the other layer reaches thin-layer limit to show potential use of such sandwich system. Analytical solutions are obtained for the first two cases and numerical solution is presented for the third case. It is found that if the thin layer is near incompressible, interfacial wrinkles can be suppressed. The equilibrium wave modes for the three limiting cases are also illustrated. The resulting solutions for the sandwich system can be reduced to the classic solutions available for a bilayer system.

Acknowledgment

The authors wish to thank the reviewers for their helpful comments.

Appendix

Boundary Value Problem of Elastic Field in Two Layers

Due to the imposed periodic displacement boundary condition at the interface between film and both layers, the Airy stress function can be separated in the form of

$$F(x,z) = f(z)\cos(kx) \tag{A1}$$

and the function satisfies

$$\nabla^2\nabla^2 F(x,z) = 0 \tag{A2}$$

Inserting Eq. (A1) to Eq. (A2), we obtain the characteristic equation

$$k^4 F - 2k^2 F^{(2)} + F^{(4)} = 0 \tag{A3}$$

where $F^{(i)}$ means i th derivative of F with respect to z. The general solution can be written as

$$\begin{aligned} F = {} & [D_1\cosh(kz) + D_2\sinh(kz) + D_3 z\cosh(kz) \\ & + D_4 z\sinh(kz)]\cos(kx) \end{aligned} \tag{A4}$$

where D_1, D_2, D_3, D_4 are coefficients to be determined by boundary condition. Using Eq. (A4), the stress components can be expressed as

$$\begin{aligned} \sigma_{xx} &= k^2\left\{D_1\cosh(kz) + D_2\sinh(kz) + D_3 z\cosh(kz) + D_4 z\sinh(kz) + \frac{2}{k}[D_3\sinh(kz) + D_4\cosh(kz)]\right\}\cos(kx) \\ \sigma_{zz} &= -k^2[D_1\cosh(kz) + D_2\sinh(kz) + D_3 z\cosh(kz) + D_4 z\sinh(kz)]\cos(kx) \\ \sigma_{xz} &= k^2\left\{D_1\sinh(kz) + D_2\cosh(kz) + D_3 z\sinh(kz) + D_4 z\cosh(kz) + \frac{1}{k}[D_3\cosh(kz) + D_4\sinh(kz)]\right\}\sin(kx) \end{aligned} \tag{A5}$$

The displacement components are obtained as

$$\begin{aligned} u &= \frac{1}{2\mu}\left\{\begin{array}{l} D_1 k\cosh(kz) + D_2 k\sinh(kz) \\ +D_3[2(1-\nu)\sinh(kz) + kz\cosh(kz)] + D_4[2(1-\nu)\cosh(kz) + kz\sinh(kz)] \end{array}\right\}\sin(kx) \\ w &= -\frac{1}{2\mu}\left\{\begin{array}{l} D_1 k\sinh(kz) + D_2 k\cosh(kz) \\ +D_3[(2\nu-1)\cosh(kz) + kz\sinh(kz)] + D_4[(2\nu-1)\sinh(kz) + kz\cosh(kz)] \end{array}\right\}\cos(kx) \end{aligned} \tag{A6}$$

The boundary conditions for lower and upper layers are listed below:

Lower layer

$$\begin{aligned} & u = w = 0 \ \text{ at } \ z = -t/2 - H_l \\ & w = A\cos(kx),\ \sigma_{xz} = 0 \ \text{ at } z = -t/2 \end{aligned} \tag{A7}$$

Upper layer

$$\begin{aligned} & u = w = 0 \ \text{ at } z = t/2 + H_u \\ & w = A\cos(kx),\ \sigma_{xz} = 0 \ \text{ at } z = t/2 \end{aligned} \tag{A8}$$

Inserting Eqs. (A5), (A6) into Eqs. (A7), (A8), D_1, D_2, D_3, D_4 are totally determined as follows:

Lower layer

$$
\begin{aligned}
D_1^{\mathrm{l}} &= \frac{M_1^{\mathrm{l}}\cosh\left(2kH_{\mathrm{l}}+\frac{kt}{2}\right)+M_2^{\mathrm{l}}\cosh\left(\frac{kt}{2}\right)+M_3^{\mathrm{l}}\sinh\left(\frac{kt}{2}\right)+M_4^{\mathrm{l}}\sinh\left(2kH_{\mathrm{l}}+\frac{kt}{2}\right)}{-2M_1^{\mathrm{l}}\sinh(2kH_{\mathrm{l}})+8kH_{\mathrm{l}}}\frac{A\overline{E}_{\mathrm{l}}}{k}\\
D_2^{\mathrm{l}} &= \frac{M_1^{\mathrm{l}}\sinh\left(2kH_{\mathrm{l}}+\frac{kt}{2}\right)+M_2^{\mathrm{l}}\sinh\left(\frac{kt}{2}\right)+M_3^{\mathrm{l}}\cosh\left(\frac{kt}{2}\right)-M_4^{\mathrm{l}}\cosh\left(2kH_{\mathrm{l}}+\frac{kt}{2}\right)}{-2M_1^{\mathrm{l}}\sinh(2kH_{\mathrm{l}})+8kH_{\mathrm{l}}}\frac{A\overline{E}_{\mathrm{l}}}{k}\\
D_3^{\mathrm{l}} &= \frac{2kH_{\mathrm{l}}\cosh\left(\frac{kt}{2}\right)-\sinh\left(\frac{kt}{2}\right)-\frac{M_1^{\mathrm{l}}}{2}\sinh\left(2kH_{\mathrm{l}}+\frac{kt}{2}\right)}{-M_1^{\mathrm{l}}\sinh(2kH_{\mathrm{l}})+4kH_{\mathrm{l}}}\frac{A\overline{E}_{\mathrm{l}}}{k}\\
D_4^{\mathrm{l}} &= \frac{2kH_{\mathrm{l}}\sinh\left(\frac{kt}{2}\right)-\cosh\left(\frac{kt}{2}\right)-\frac{M_1^{\mathrm{l}}}{2}\cosh\left(2kH_{\mathrm{l}}+\frac{kt}{2}\right)}{-M_1^{\mathrm{l}}\sinh(2kH_{\mathrm{l}})+4kH_{\mathrm{l}}}\frac{A\overline{E}_{\mathrm{l}}}{k}
\end{aligned}
\tag{A9}
$$

Upper layer

$$
\begin{aligned}
D_1^{\mathrm{u}} &= \frac{M_1^{\mathrm{u}}\cosh\left(2kH_{\mathrm{u}}+\frac{kt}{2}\right)+M_2^{\mathrm{u}}\cosh\left(\frac{kt}{2}\right)+M_3^{\mathrm{u}}\sinh\left(\frac{kt}{2}\right)+M_4^{\mathrm{u}}\sinh\left(2kH_{\mathrm{u}}+\frac{kt}{2}\right)}{2M_1^{\mathrm{u}}\sinh(2kH_{\mathrm{l}})-8kH}\frac{A\overline{E}_{\mathrm{u}}}{k}\\
D_2^{\mathrm{u}} &= \frac{M_1^{\mathrm{u}}\sinh\left(2kH_{\mathrm{u}}+\frac{kt}{2}\right)+M_2^{\mathrm{u}}\sinh\left(\frac{kt}{2}\right)+M_3^{\mathrm{u}}\cosh\left(\frac{kt}{2}\right)+M_4^{\mathrm{u}}\cosh\left(2kH_{\mathrm{u}}+\frac{kt}{2}\right)}{-2M_1^{\mathrm{u}}\sinh(2kH_{\mathrm{u}})+8kH_{\mathrm{u}}}\frac{A\overline{E}_{\mathrm{u}}}{k}\\
D_3^{\mathrm{u}} &= \frac{2kH_{\mathrm{u}}\cosh\left(\frac{kt}{2}\right)-\sinh\left(\frac{kt}{2}\right)-\frac{M_1^{\mathrm{u}}}{2}\sinh\left(2kH_{\mathrm{u}}+\frac{kt}{2}\right)}{-M_1^{\mathrm{u}}\sinh(2kH_{\mathrm{u}})+4kH_{\mathrm{u}}}\frac{A\overline{E}_{\mathrm{u}}}{k}\\
D_4^{\mathrm{u}} &= \frac{2kH_{\mathrm{u}}\sinh\left(\frac{kt}{2}\right)-\cosh\left(\frac{kt}{2}\right)-\frac{M_1^{\mathrm{u}}}{2}\cosh\left(2kH_{\mathrm{u}}+\frac{kt}{2}\right)}{M_1^{\mathrm{u}}\sinh(2kH_{\mathrm{u}})-4kH_{\mathrm{u}}}\frac{A\overline{E}_{\mathrm{u}}}{k}\\
M_1^r &= 6-8\nu_r,\quad M_2^r = 10-24\nu_r+16\nu_r^2+2H_rk^2t+4(kH_r)^2\\
M_3^r &= -k(4H_r+t),\quad M_4^r = -kt(3-4\nu_r),(r=l,\ u)
\end{aligned}
\tag{A10}
$$

in which subscript l and u indicates lower layer and upper layer. $\overline{E}=(E/1-\nu^2)$ is the plane strain modulus. Hence, the interfacial pressure can be evaluated by substituting Eqs. (A9) and (A10) into Eq. (A5)

$$
\begin{aligned}
p_{\mathrm{l}} &= \sigma_{zz}^{\mathrm{l}}\big|_{z=-t/2} = g_{\mathrm{l}}kw\overline{E}_{\mathrm{l}},\\
p_{\mathrm{u}} &= \sigma_{zz}^{\mathrm{u}}\big|_{z=t/2} = g_{\mathrm{u}}kw\overline{E}_{\mathrm{u}}
\end{aligned}
\tag{A11}
$$

where

$$
\begin{aligned}
g_{\mathrm{l}} &= -\left[D_1^{\mathrm{l}}\cosh\left(\frac{kt}{2}\right)-D_2^{\mathrm{l}}\sinh\left(\frac{kt}{2}\right)-D_3^{\mathrm{l}}\frac{t}{2}\cosh\left(\frac{kt}{2}\right)\right.\\
&\quad\left.+D_4^{\mathrm{l}}\frac{t}{2}\sinh\left(\frac{kt}{2}\right)\right]\left(\frac{A\overline{E}_{\mathrm{l}}}{k}\right)^{-1}\\
g_{\mathrm{u}} &= -\left[D_1^{\mathrm{u}}\cosh\left(\frac{kt}{2}\right)+D_2^{\mathrm{u}}\sinh\left(\frac{kt}{2}\right)+D_3^{\mathrm{u}}\frac{t}{2}\cosh\left(\frac{kt}{2}\right)\right.\\
&\quad\left.+D_4^{\mathrm{u}}\frac{t}{2}\sinh\left(\frac{kt}{2}\right)\right]\left(\frac{A\overline{E}_{\mathrm{u}}}{k}\right)^{-1}
\end{aligned}
\tag{A12}
$$

References

[1] Bowden, N., Brittain, S., Evans, A. G., Hutchinson, J. W., and Whitesides, G. M., 1998, "Spontaneous Formation of Ordered Structures in Thin Films of Metals Supported on an Elastomeric Polymer," Nature, **393**(6681), pp. 146–149.

[2] Chan, E. P., and Crosby, A. J., 2006, "Spontaneous Formation of Stable Aligned Wrinkling Patterns," Soft Matter, **2**(4), pp. 324–328.

[3] Genzer, J., and Groenewold, J., 2006, "Soft Matter With Hard Skin: From Skin Wrinkles to Templating and Material Characterization," Soft Matter, **2**(4), pp. 310–323.

[4] Huck, W. T., Bowden, N., Onck, P., Pardoen, T., Hutchinson, J. W., and Whitesides, G. M., 2000, "Ordering of Spontaneously Formed Buckles on Planar Surfaces," Langmuir, **16**(7), pp. 3497–3501.

[5] Moon, M. W., Lee, S. H., Sun, J. Y., Oh, K. H., Vaziri, A., and Hutchinson, J. W., 2007, "Wrinkled Hard Skins on Polymers Created by Focused Ion Beam," Proc. Natl. Acad. Sci. USA, **104**(4), pp. 1130–1133.

[6] Li, B., Cao, Y.-P., Feng, X.-Q., and Gao, H., 2012, "Mechanics of Morphological Instabilities and Surface Wrinkling in Soft Materials: A Review," Soft Matter, **8**(21), pp. 5728–5745.

[7] Gioia, G., and Ortiz, M., 1997, "Delamination of Compressed Thin Films," *Advances in Applied Mechanics*, Vol. 33, J. W. Hutchinson, and T. Y. Wu, eds., Academic Press, San Diego, CA, pp. 119–192.

[8] Hutchinson, J. W., 2001, "Delamination of Compressed Films on Curved Substrates," J. Mech. Phys. Solids, **49**(9), pp. 1847–1864.

[9] Yin, H., Huang, R., Hobart, K. D., Suo, Z., Kuan, T. S., Inoki, C. K., Shieh, S. R., Duffy, T. S., Kub, F. J., and Sturm, J. C., 2002, "Strain Relaxation of SiGe Islands on Compliant Oxide," J. Appl. Phys., **91**(12), pp. 9716–9722.

[10] Khang, D.-Y., Rogers, J. A., and Lee, H. H., 2009, "Mechanical Buckling: Mechanics, Metrology, and Stretchable Electronics," Adv. Funct. Mater., **19**(10), pp. 1526–1536.

[11] Kim, D. H., Ahn, J. H., Choi, W. M., Kim, H. S., Kim, T. H., Song, J., Huang, Y., Liu, Z., Lu, C., and Rogers, J. A., 2008, "Stretchable and Foldable Silicon Integrated Circuits," Science, **320**(5875), pp. 507–511.

[12] Rogers, J. A., Someya, T., and Huang, Y., 2010, "Materials and Mechanics for Stretchable Electronics," Science, **327**(5973), pp. 1603–1607.

[13] Jiang, H., Khang, D.-Y., Song, J., Sun, Y., Huang, Y., and Rogers, J. A., 2007, "Finite Deformation Mechanics in Buckled Thin Films on Compliant Supports," Proc. Natl. Acad. Sci. USA, **104**(40), pp. 15607–15612.

[14] Jiang, H., Khang, D.-Y., Fei, H., Kim, H., Huang, Y., Xiao, J., and Rogers, J. A., 2008, "Finite Width Effect of Thin-Films Buckling on Compliant Substrate: Experimental and Theoretical Studies," J. Mech. Phys. Solids, **56**(8), pp. 2585–2598.
[15] Song, J., Jiang, H., Liu, Z. J., Khang, D. Y., Huang, Y., Rogers, J. A., Lu, C., and Koh, C. G., 2008, "Buckling of a Stiff Thin Film on a Compliant Substrate in Large Deformation," Int. J. Solids Struct., **45**(10), pp. 3107–3121.
[16] Song, J., Huang, Y., Xiao, J., Wang, S., Hwang, K. C., Ko, H. C., Kim, D. H., Stoykovich, M. P., and Rogers, J. A., 2009, "Mechanics of Noncoplanar Mesh Design for Stretchable Electronic Circuits," J. Appl. Phys., **105**(12), p. 123516.
[17] Breid, D., and Crosby, A. J., 2009, "Surface Wrinkling Behavior of Finite Circular Plates," Soft Matter, **5**(2), pp. 425–431.
[18] Yoo, P. J., and Lee, H. H., 2008, "Complex Pattern Formation by Adhesion-Controlled Anisotropic Wrinkling," Langmuir, **24**(13), pp. 6897–6902.
[19] Chan, E. P., Smith, E. J., Hayward, R. C., and Crosby, A. J., 2008, "Surface Wrinkles for Smart Adhesion," Adv. Mater., **20**(4), pp. 711–716.
[20] Chan, E. P., and Crosby, A. J., 2006, "Fabricating Microlens Arrays by Surface Wrinkling," Adv. Mater., **18**(24), pp. 3238–3242.
[21] Chung, J. Y., Nolte, A. J., and Stafford, C. M., 2011, "Surface Wrinkling: A Versatile Platform for Measuring Thin-Film Properties," Adv. Mater., **23**(3), pp. 349–368.
[22] Stafford, C. M., Harrison, C., Beers, K. L., Karim, A., Amis, E. J., VanLandingham, M. R., Kim, H. C., Volksen, W., Miller, R. D., and Simonyi, E. E., 2004, "A Buckling-Based Metrology for Measuring the Elastic Moduli of Polymeric Thin Films," Nature Mater., **3**(8), pp. 545–550.
[23] Chen, X., and Hutchinson, J. W., 2004, "A Family of Herringbone Patterns in Thin Films," Scr. Mater., **50**(6), pp. 797–801.
[24] Chen, X., and Hutchinson, J. W., 2004, "Herringbone Buckling Patterns of Compressed Thin Films on Compliant Substrates," ASME J. Appl. Mech., **71**(5), pp. 597–603.
[25] Yoo, P., and Lee, H., 2003, "Evolution of a Stress-Driven Pattern in Thin Bilayer Films: Spinodal Wrinkling," Phys. Rev. Lett., **91**(15), p. 154502.
[26] Yoo, P., Suh, K., Kang, H., and Lee, H., 2004, "Polymer Elasticity-Driven Wrinkling and Coarsening in High Temperature Buckling of Metal-Capped Polymer Thin Films," Phys. Rev. Lett., **93**(3), p. 034301.
[27] Cai, S., Breid, D., Crosby, A. J., Suo, Z., and Hutchinson, J. W., 2011, "Periodic Patterns and Energy States of Buckled Films on Compliant Substrates," J. Mech. Phys. Solids, **59**(5), pp. 1094–1114.
[28] Audoly, B., and Boudaoud, A., 2008, "Buckling of a Stiff Film Bound to a Compliant Substrate—Part I," J. Mech. Phys. Solids, **56**(7), pp. 2401–2421.
[29] Cerda, E., and Mahadevan, L., 2003, "Geometry and Physics of Wrinkling," Phys. Rev. Lett., **90**(7), p. 074302.
[30] Cerda, E., Ravi-Chandar, K., and Mahadevan, L., 2002, "Thin Films—Wrinkling of an Elastic Sheet Under Tension," Nature, **419**(6907), pp. 579–580.
[31] Huang, R., and Suo, Z., 2002, "Wrinkling of a Compressed Elastic Film on a Viscous Layer," J. Appl. Phys., **91**(3), pp. 1135–1142.
[32] Huang, R., and Suo, Z., 2002, "Instability of a Compressed Elastic Film on a Viscous Layer," Int. J. Solids Struct., **39**(7), pp. 1791–1802.
[33] Im, S., and Huang, R., 2008, "Wrinkle Patterns of Anisotropic Crystal Films on Viscoelastic Substrates," J. Mech. Phys. Solids, **56**(12), pp. 3315–3330.
[34] Im, S. H., and Huang, R., 2005, "Evolution of Wrinkles in Elastic-Viscoelastic Bilayer Thin Films," ASME J. Appl. Mech., **72**(6), pp. 955–961.
[35] Huang, R., 2005, "Kinetic Wrinkling of an Elastic Film on a Viscoelastic Substrate," J. Mech. Phys. Solids, **53**(1), pp. 63–89.
[36] Cheng, H., Zhang, Y., Hwang, K.-C., Rogers, J. A., and Huang, Y., "Buckling of a Stiff Thin Film on a Pre-Strained Bi-Layer Substrate," Int. J. Solids Struct., **51**(18), pp. 3113–3118.
[37] Allen, H. G., 1969, *Analysis and Design of Structured Sandwich Panels*, Pergamon, New York.
[38] Niu, K., and Talreja, R., 1999, "Modeling of Wrinkling in Sandwich Panels Under Compression," J. Eng. Mech., **125**(8), pp. 875–883.
[39] Birman, V., 2004, "Wrinkling of Composite-Facing Sandwich Panels Under Biaxial Loading," J. Sandwich Struct. Mater., **6**(3), pp. 217–237.
[40] Laudau, L. D., and Lifshitz, E. M., 1959, *Theory of Elasticity*, Pergamon, London.
[41] Huang, Z. Y., Hong, W., and Suo, Z., 2005, "Nonlinear Analyses of Wrinkles in a Film Bonded to a Compliant Substrate," J. Mech. Phys. Solids, **53**(9), pp. 2101–2118.